JETIR.ORG ISSN: 2349-5162 | ESTD Year : 2014 | Monthly Issue
JOURNAL OF EMERGING TECHNOLOGIES AND INNOVATIVE RESEARCH (JETIR)
An International Scholarly Open Access, Peer-reviewed, Refereed Journal

GREEN SYNTHESIS AND PHYTOCHEMICAL CHARACTERIZATION OF SILVER NANOPARTICLES FROM LEAF EXTRACTS OF *CHAMAECOSTUS CUSPIDATUS* (NEES & MART)

[1]Bibi Hafsa Azra, [2]Dr.N. Lakshmi Bhavani

[1]Research Scholar, [2]Associate professor

Department of Botany

University College of Science, Saifabad, Hyderabad, India

Abstract: The current study employs *C.cuspidatus* leaf extract to make silver nanoparticles simplistic and environmental friendly. Plants are employed as remedies in many traditions and serve as a source of potent pharmaceuticals for the pharmaceutical industry due to specific bioactive chemicals. Silver nanoparticles (AgNPs) are progressively used in various industries, including medicine, food, health care, consumer goods, and industry, due to their unique physical and chemical properties. The phytochemical screening analysis of the silver nanoparticles from leaf extract showed some significant components present in it, whereas GC-MS analysis indicated a plethora of organic silicon compounds and carboxylic acids. The biosynthesized AgNPs were characterized by U.V., FTIR, SEM, XRD, Zeta potential and particle size analysis. The characterization results revealed that nanoparticles have a spherical form, with an average particle size of 236.0nm, a particle charge of 0.1mv and a cubic crystalline structure.

Keywords: Silver nanoparticles (AgNPs), XRD, SEM, Zeta potential

I. INTRODUCTION

Plants are employed as remedies in many traditions and serve as a source of potent pharmaceuticals for the pharmaceutical industry due to specific bioactive chemicals. *Chamaecostus cuspidatus*, commonly known as the insulin plant, belongs to Costaceae. As the study progresses, a new aspect of silver nanoparticles has shown to be highly efficient in analytical studies. Silver nanoparticles (AgNPs) are increasingly utilized in various industries, including medicine, food, health care, consumer goods, and industry, due to their unique physical and chemical properties. They have been used as antibacterial agents in the industrial, household, and healthcare-related products, in consumer products, medical device coatings, optical sensors, and cosmetics, in the pharmaceutical and food industries, in diagnostics, orthopedics, drug delivery, and as anticancer agents, and have ultimately enhanced the tumour-killing effects of anticancer drugs (Zhang et al. 2016). Due to its cutting-edge character and broad application range in practically every research and technology department, including biomedical sciences, nanobiotechnology, which deals with metal nanoparticles, has attracted increasing attention (Jyoti et al. 2016).

Silver nanoparticles can continuously discharge silver ions, a microbe-killing mechanism. Silver ions can cling to the cell wall and cytoplasmic membrane due to electrostatic attraction and affinity for sulphur proteins. Silver nanoparticles are made up of 20 to 15,000 silver atoms and have a diameter of fewer than 100 nanometers. Silver nanoparticles display extraordinary antibacterial action due to their substantial surface-to-volume ratio, even at low concentrations (Yin et al., 2020).

This analysis explores the phytochemical and GC-MS analysis of silver nanoparticle leaf extract from Chamaecostus cuspidatus and their characterization. In this study, silver nanoparticles were synthesized utilizing a green chemistry

technique using *C.cuspidatus* leaf extract, and the nanoparticles were characterized using FTIR, UV XRD, SEM, Zeta potential, and PSA analysis.

II. MATERIALS AND METHODS

2.1 Preparation of Leaf Extract for silver nanoparticles

At first, fresh *C. cuspidatus* leaves were collected and rinsed with tap water. The surface was thoroughly cleaned with distilled water under running water until no contaminants remained. The fresh leaves were then cut into small pieces, weighed, and combined with 100 mL of distilled water in a beaker. The mixture was boiled at 60°C for 20 minutes, stirring regularly, before cooling to room temperature. The blend was filtered using Whatman 42 filter paper and centrifuged for 20 minutes. The extract was kept in the fridge until it was needed to make Ag nanoparticles from an AgNO3 precursor solution (Aritonang et al., 2019).

2.2 Preparation of silver nanoparticles

In an Erlenmeyer flask, the 5 mL filtrate was treated with a 45 mL aqueous one mM silver nitrate (AgNo3) solution and incubated at room temperature, yielding a brownish yellow solution suggesting AgNP production. The AgNP solution was then purified by centrifugation three times for 20 minutes at 15,000 rpm. The pellet dispersed in deionized water after removing the supernatant (Sinha & Paul, 2015).

2.3 Phytochemical analysis (Method adopted by Srinivas R. et al., 2014)

2.3.1 Test for tannins

In 2ml of distilled water, a few drops of ferric chloride solution were added to roughly 2ml of extract. The appearance of green-tinted precipitate confirms the presence of tannins.

2.3.2 Test for saponins

In a test tube, 3ml of the extract was mixed with 3ml of distilled water and vigorously shaken for a few moments. The test tube was heated, and creating a stable foam indicates the presence of saponins.

2.3.3 Test for flavonoids

1ml of 10 percent lead acetate solution was added to 1ml of extract in a test tube. The appearance of the yellow precipitate can determine the presence of flavonoids.

2.3.4 Test for Alkaloids

On a hot water bath, 3ml of the extract was mixed with 3ml of 1% HCL. Then 1ml of the liquid was split between two test tubes. 1ml of Mayer's reagent was added to the second test tube. The formation of a buff-coloured precipitate can confirm the presence of alkaloids.

2.3.5 Test for terpenoids

2 mL extract was dissolved in 2 mL $CHCl_3$ and evaporated to dryness. After that, 2 mL of concentrated sulphuric acid (H2SO4) was added and heated for about 2 minutes. The emergence of a greyish colour indicates the presence of terpenoids.

2.3.6 Test for steroids

Two tests were carried out to perceive the presence of steroids in the extract, and those were the Salkowski's test and the Liebermann test.

Salkowski's test: 2 mL organic extract diluted in 2 mL chloroform; to this, 2 mL concentrated H2So4 was added. The emergence of red colour in the chloroform section indicates the presence of steroids.

2.3.7 Test for Phenols

5ml distilled water was added to 1gm of extract, and the solution was then treated with a 5% ferric chloride solution. The presence of phenols was validated by forming a dark green colour.

2.4 GC-MS Analysis of $AgNo_3$ *C.cuspidatus* leaf extract

The GC-MS analysis of *C.cuspidatus* extracts was performed using a GCMS-QP2010SE SHIMADZU, Japan, bonded with an optima 5 ms capillary column with a 0.25 m film thickness described by Ajiboye et al. with slight adjustments. The following were the gas chromatography conditions: initial column oven temperature (60°C) programmed to hike to 160°C at a frequency of 10°C/min and subsequently to 250°C with a hold duration of 2 min/increment, and an injection volume of 0.5µL in the splitless method with a split ratio of 1:1 and injector temperature set at 200° C (Azra & Laxmi, 127). The mass spectrophotometer settings were as follows: 230°C for the ion source, 250°C for the interface, 4.5 min for the solvent delay, and a scan range of 50–700 amu. The electron ionization mode and multiplier voltage changed to 70 eV and 1859 V. To identify unknown components in the extracts, the retention time, fragmentation pattern, and mass spectral data compared to those in the Wiley and National Institute Standards and Technology (NIST) libraries (Iheagwam et al. 2019).

2.5 Characterization of $AgNo_3$ leaf extract of *C.cuspidatus*

2.5.1 UV-Vis Spectroscopy

The bioreduction of Ag+ ions in solutions was examined by measuring the U.V.–vis spectra of the reaction medium at room temperature using a UV 1800 series spectrophotometer with a resolution of 1 nm in the 190-1100 nm range. Absorbance can be calculated from percent transmittance (%T) using this formula:

Absorbance = 2 – log(%T)

2.5.2 FTIR

On a Shimadzu FTIR Spectrometer, potential functional groups in biomolecules present in the plant extract were detected using Fourier Transform Infrared Spectroscopy (FTIR). The AgNPs solution was centrifuged for 30 minutes at 12,000 rpm for FTIR. The pellet was washed three times with 25 mL of deionized water to remove any free proteins or enzymes that were not capping the AgNPs (Jyoti et al., 218).

2.5.3 SEM

The SIGMA model, CASL ZEISS, German) was used for scanning electron microscopic (SEM) investigation at a 10 kV accelerating voltage. The sample was prepared on a carbon-coated copper grid by putting a minimal amount of the sample on the grid and blotting the excess solution away using blotting paper. After that, the film was left to cure for 5 minutes under a mercury lamp (Muthukrishan et al., 2015).

2.5.4 Particle size

The particle size distribution and surface charge of AgNPs were determined using a particle size analyzer (Zetasizer nano Z.S., Malvern Instruments Ltd., U.K.) at 25 C with 90^0 C detection angle. More than 500 particles were counted to obtain the particle size data. Data about particle size and size distribution can be represented in either a tabular or a graphical representation (Akbari et al., 2011).

The Z average is the ensemble collection of particles' intensity weighted mean hydrodynamic size as measured by dynamic light scattering (DLS). The polydispersity index (P.I.) is a size-based measure of a sample's heterogeneity. Polydispersity can occur due to a sample's size distribution, agglomeration, or aggregation during isolation or analysis (Mudalige, 2019).

2.5.5 Zeta potential

The zeta potential is used to depict the surface charge and stability of S-AgNPs. Nanoparticles with a zeta potential of -10 to +10 mV are regarded as neutral, but nanoparticles with a zeta potential of greater than +30 mV or less than -30 mV are firmly cationic and strongly anionic, respectively (Singh et al., 365). The zetametry readings were performed at 2.2V and 25.1 °C on a Horiba sz-100 with the conductivity set at 9.606 mS/cm and the conductivity set at 9.606 mS/cm.

2.5.6 XRD

Leaf extracts containing silver nanoparticles were lyophilized and pulverized for use in XRD analysis. The diffracted intensities were measured at two angles and ranged from 10 to 80 (Muthukrishnan et al., 2015). The Debye–Scherrer equation was used to calculate the size of the AgNPs.

Scherrer Formula

$$Dp = (0.94 \times \lambda) / (\beta \times \cos\theta)$$

Where, Dp = Average Crystallite size, β = Line broadening in radians, θ = Bragg angle, λ = X-Ray wavelength

The distance between the curve points at the peak half maximum level is known as the Full width at half maximum (FWHM). Draw a vertical line from the peak maximum to the baseline on a data graph. To locate the centre of the line, multiply the length of the line by two.

III. RESULTS & DISCUSSION

The characterization of nanoparticles is critical for understanding and managing nanoparticle manufacturing and uses. Scanning electron microscopy (SEM), U.V.–vis spectroscopy, powder X-ray diffractometry (XRD), and Fourier transform infrared spectroscopy are some of the techniques used to characterize materials (FTIR) (Muthukrishan et al., 2015). Using these techniques, different parameters such as particle range, character, crystallinity, fractal dimensions, pore size, and surface area are determined. Researchers have focused increasing attention on the green products and applications of AgNPs utilizing various plant extracts in the last year.

3.1 Phytochemical analysis of $AgNo_3$ leaf extract

According to a phytochemical study, the bulk of secondary metabolites is present in AgNPs leaf extract of *C.cuspidatus*, although flavonoids and terpenoids are absent. As validated by the FTIR spectrum, alkaloids, phenols, and tannins were found in synthesized AgNPs, which may be responsible for the efficient capping and stabilization of nanoparticles.

Table -1: Phytochemical analysis of agnps of c.cuspidatus

Test	AgNPs Extract
Test for Tannins	Present
Test for Saponins	Present
Test for Flavonoids	Absent

Test for Alkaloids	Present
Test for Terpenoids	Absent
Test fo Steroids	Present
Test for Phenols	Present

3.2 GC-MS analysis of $AgNo_3$ leaf extract

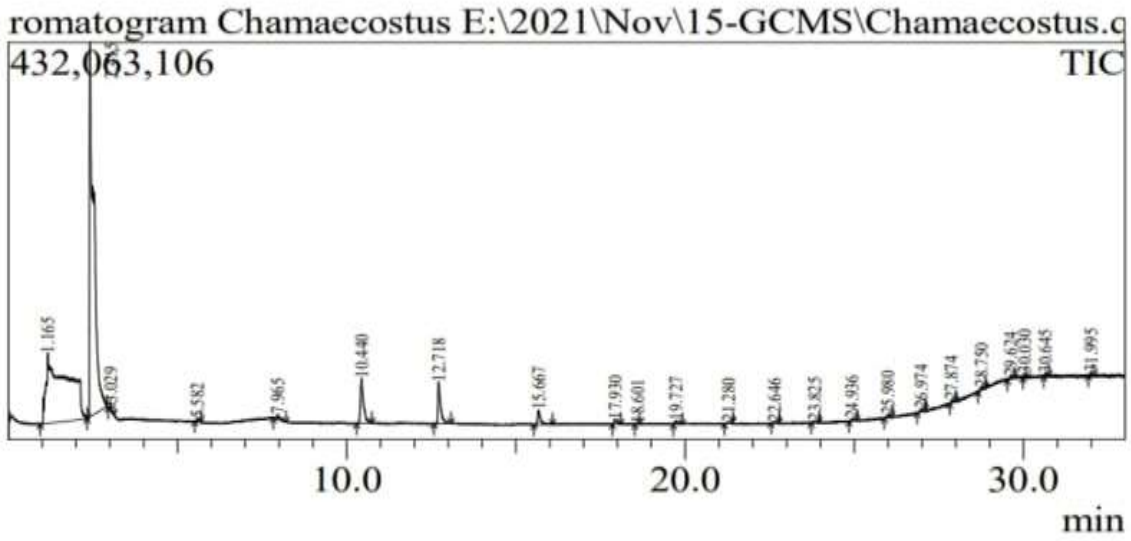

Fig- 1: GC-MS analysis graph

Table – 2: GC-MS analysis of aqueous AgNPs extract of C.cuspidatus

S.No	Name of the compound	Mol.For	Mol. Wt	Retention time	Area %	Nature of Compound
1.	Thiazolidinedion	C3H3NO2S	117	1.165	42.45	Hetero cyclic compound
2.	Cyclotrisiloxane	$C_6H_{18}O_3Si_3$	222	3.029	0.03	Organic Silicon compounds
3.	Cyclotetrasiloxane	$C_8H_{24}O_4Si_4$	296	5.582	0.15	Organic Silicon compounds
4.	Cyclohexasiloxane	C12H36O6Si6	444	10.440	4.01	Organic Silicon compounds
5.	Cycloheptasiloxane	C14H42O7Si7	518	12.718	3.23	Organic Silicon compounds
6.	Cyclooctasiloxane	C16H48O8Si8	592	15.667	1.17	Organic Silicon compounds
7.	Heptasiloxane	C16H48O6Si7	532	17.930	0.33	Organic Silicon compounds
8.	1,1-Cyclopropanedicarboxamide	C5H8N2O2	128	18.601	0.05	Carboxylic acid
9.	Octasiloxane	C16H50O7Si8	578	22.646	0.04	Organic Silicon compounds

10.	Heptasiloxane	C16H48O6Si7	532	23.825	0.09	Organic Silicon compounds
11.	Cyclodecasiloxane	C20H60O10Si10	740	30.645	0.05	Organic Silicon compounds
12.	2,3-Dimethoxyphenyllactic acid	C17H30O5Si2	370	31.995	0.02	Organic Compound

The bioactive components found in the aqueous silver nanoparticle leaf extract of C.cuspidatus were identified by GC-MS analysis. Numerous chemicals were found based on the data presented, most of which are organic silicon compounds and carboxylic acid heterocyclic compounds. The major pharmaceutical category utilized to increase insulin sensitivity in treating type 2 diabetes is called "Thiazolidinedion," also known as glitazones. Thiazolidinediones are sulphur-containing pentacyclic chemicals found in various forms throughout nature. Anti-malarial, antibacterial, anti-mycobacterium, anticancer, anti-inflammatory, antioxidant, anti-HIV (human immunodeficiency virus), and antitubercular agents contain the thiazolidinedione nucleus (Sucheta et al., 2017).

3.3 UV-Vis Spectroscopy

The synthesis of AgNPs in an aqueous solution was monitored by taking absorption spectra in the 190 - 1100 nm wavelength range. There are three significant peaks between 192 and 210 nm: 3.938, 3.951, and 4.000. As a result, a peak at the exact location indicates that the nanoparticles are the same size. The absorbance of the produced nanoparticles at each wavelength is represented by the peaks in the UV-Visible spectroscopy spectrum.

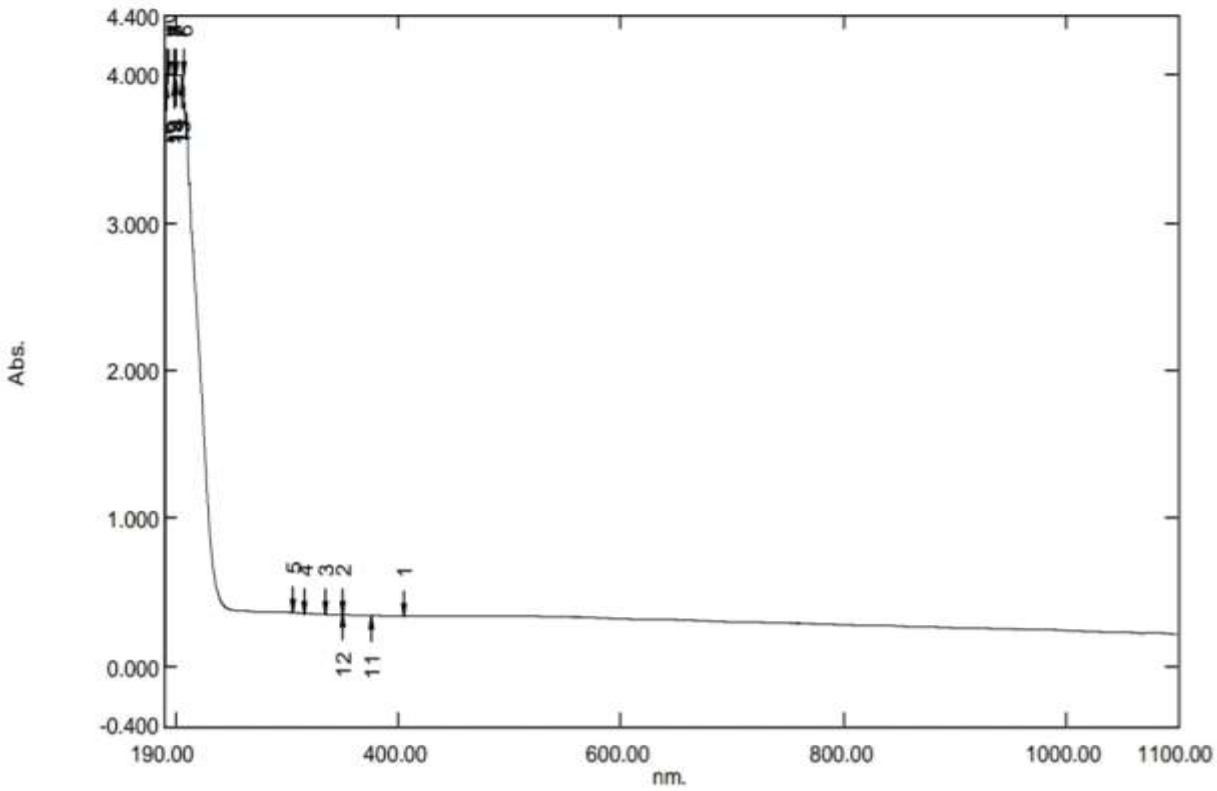

Fig -2: UV-VIS Graph

Table -3: UV-VIS analysis

Wavelength	Abs.sp	T%
404.30	**0.342**	**0.45499**
334.10	**0.353**	**0.44361**
305.30	**0.366**	**0.43053**
206.50	**4.000**	**0.0001**
198.90	**4.000**	**0.0001**
193.10	**4.000**	**0.0001**
191.30	**4.000**	**0.0001**
205.30	**3.952**	**0.00011**

199.60	**3.959**	**0.00011**
198.40	**3.951**	**0.00011**
192.50	**3.938**	**0.00012**

3.4 FTIR

FTIR was used to characterize the plant extract and the silver nanoparticles. The existence of different functional groups in biomolecules responsible for the bioreduction of Ag and the capping/stabilization of silver nanoparticles was determined using FTIR measurements. The functional groups were identified by comparing the observed intensity bands to average values. The bands in the spectra at 3446.91-3421.83 correspond to O-H stretching vibrations, which indicate the presence of alcohol and phenol. Bands generated from C-H stretching of alkanes were detected at 2933.83. the band at 1313.57 shows the presence of phenols with O-H bending.

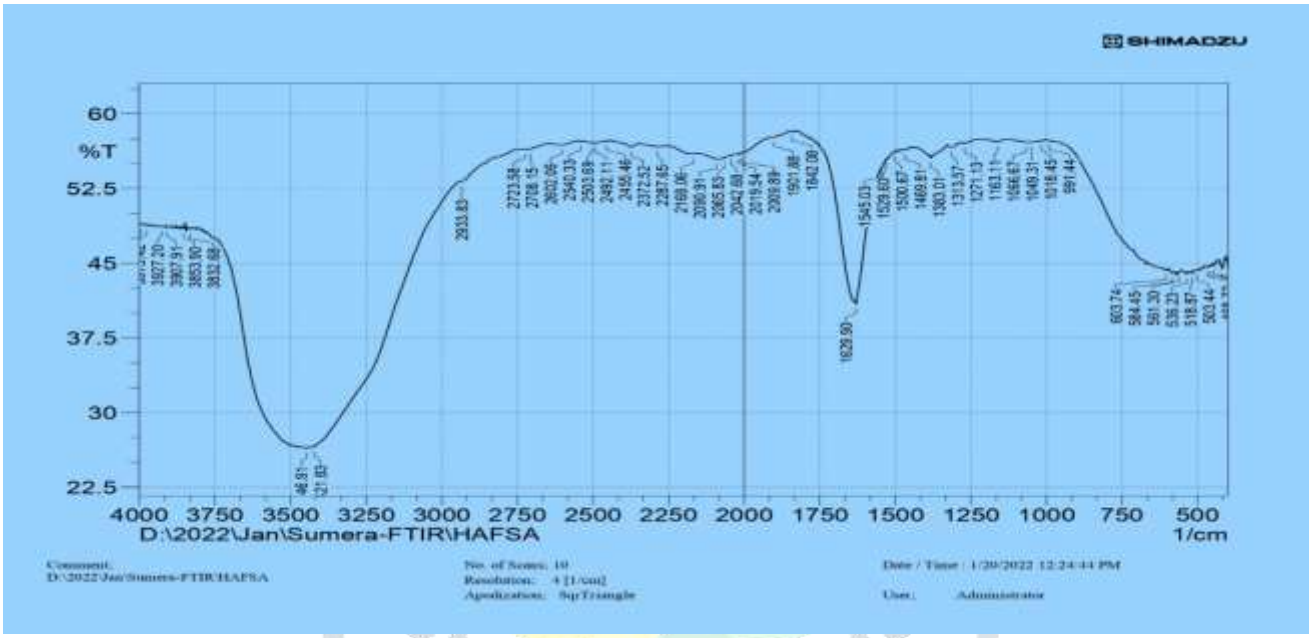

Fig- 3: FTIR spectra of aqueous AgNPS

Table -4: Readings based on FTIR analysis

Wavenumber (cm^{-1})	Compound class	Group/ Appearance
3446.91- 3421.83	Alcohol	O-H Stretching / Strong
2933.83	Alkane	C-H Stretching / Medium
2723.58- 2708.15	Aldehyde	C-H Stretching / Medium
2168.06	Thiocyanate	S-CΞN stretching/ Strong
2090.91-2009.89	isothiocyanate	N=C=S stretching / Strong
1901.88 - 1842.08	aromatic compound	C-H bending / Weak
1545.03 - 1500.67	nitro compound	N-O stretching / Strong
1383.01	Alkane or Aldehyde	C-H bending / Medium
1313.57	phenol	O-H bending / Medium
1271.13	aromatic amine	C-N stretching / Strong
1163.11- 1049.31	amine	C-N stretching / Medium
991.44	alkene	C=C bending / Strong
603.74 - 518.87	halo compound	C-Br stretching / Strong
503.44	halo compound	C-I stretching / Strong

3.5 SEM

The results show that AgNPs were predominantly uniform in size, and the shape of the particles was predicted. The percentage of resulting nanoparticles was spherical and in the size of 100 - 155 nm. The surface deposited silver

nanoparticles are seen clearly at a higher magnification in silver nitrate treated *C. cuspidatus* leaf extract. In silver nitrate treated C.cuspidatus extract, silver nanoparticles' surface deposited may be observed at greater magnification.

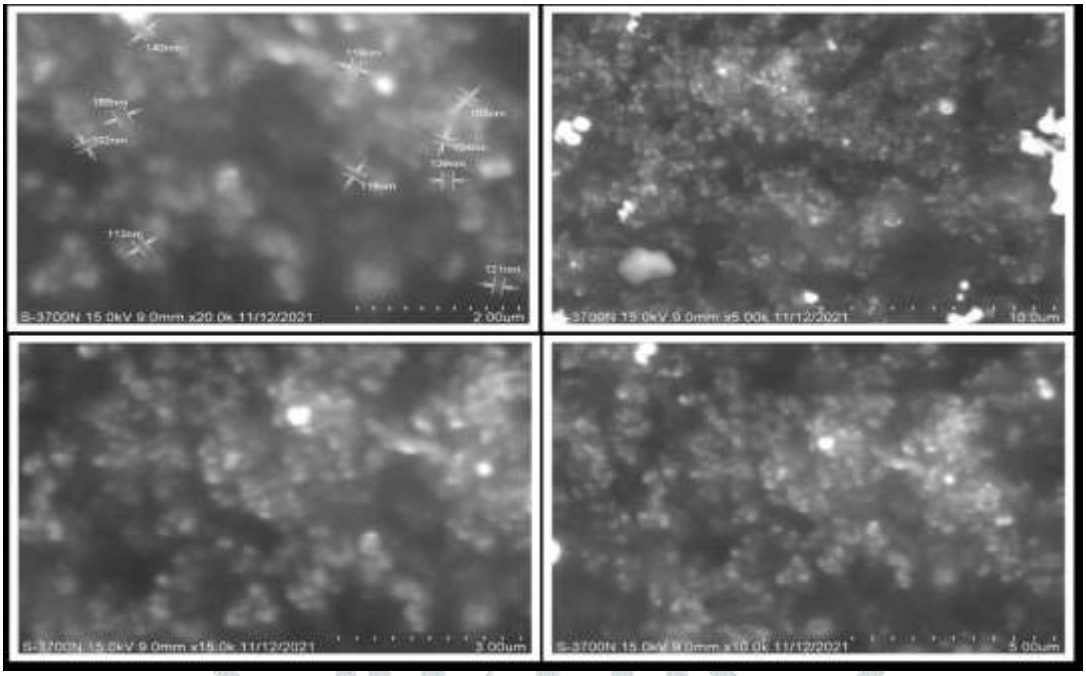

Fig -4: Sem micrographs showing spherical nanoparticles

3.6 Particle size

Table 5: Particle size distribution

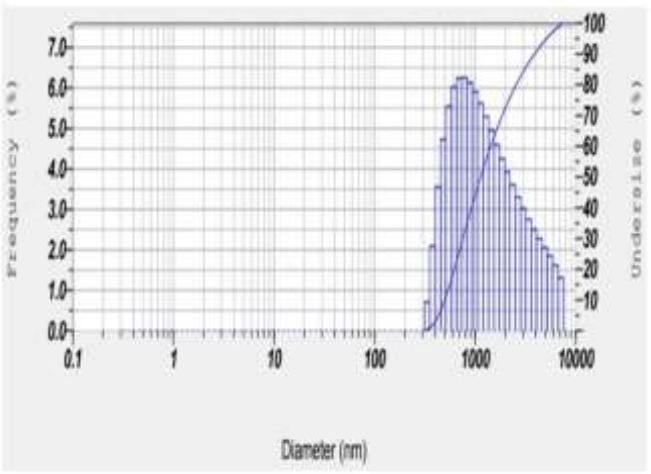

Result

Peak No	1
S.P.Area Ratio	1.00
Mean	1711.0 nm
Median	1137.0 nm
Mode	786.7 nm
Standard deviation	1482.4
Z-average	236.0 nm
PI	2.769
Count	94 KCPS
Minimum	5.0 nm
Maximum	90.0 nm

Fig-5: Particle size distribution

The particle size distribution was plotted using the particle size data in table 5. The particle size's mean, median and mode are calculated, and the Z-average and polydispersity index is also stated. The number of frequency histograms of particle size data on a linear scale is shown in Figure 5. If enough particles are counted, and the size interval is at least 10, the smooth curve formed through the histogram is a valid size-frequency curve. Hundreds of particles should be measured to get statistically reliable mean size data. The polydispersity index of nanoparticles was **2.769**, which indicates the aggregation of the particles.

3.7 Zeta potential

The surface charge and stability of S-AgNPs are depicted using the zeta potential. A value of 0.1mV for the zeta potential and electrophoretic value is nil. This zeta potential value is deemed moderately stable if it falls between 50 and +50 mV, indicating that the synthesized S-AgNPs were moderately stable in nature. The linear graph is depicted in the image, with zeta potential (mV) values on the X-axis and intensity on the y-axis.

Table 6: Zeta potential

Peak No	Zeta Potential	Electrophoretic
1.	0.1 mv	0.000000 cm2/v2
2.	___	___ cm2/v2

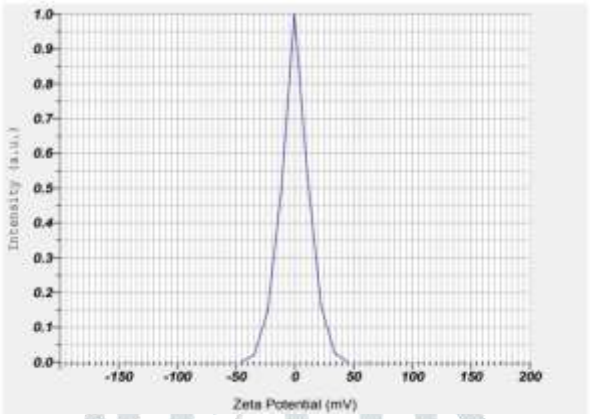

Fig-6: Zeta potential graph

3.8 XRD

X-ray crystallography revealed the crystalline nature of nanoparticles—the synthesized AgNPs' XRD pattern. The XRD pattern of silver nanoparticles showed four peaks at 2θ (Fig. 7) corresponding to (17.224), (19.126), (29.780), and (32.319) planes of standard XRD peak of silver crystals. Two high peaks in 29.780 ◦ and 32.319◦ and this characteristic structural pattern confirms that the AgNPs have a cubic crystalline structure. The XRD pattern of green synthesized AgNPs corresponded to 29.780 ◦ and 32.319◦ of cubic crystalline silver, while other peaks have a broad humped peak.

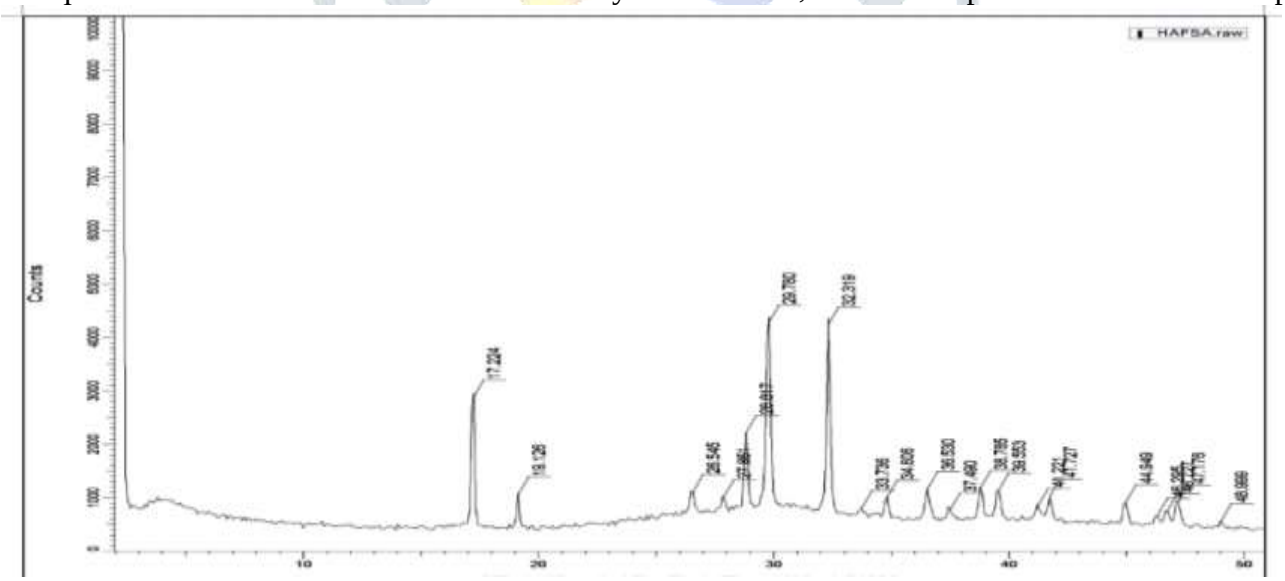

Fig- 7: XRD pattern

Table 7: XRD D-values

2θ	FWHM	Crystalline size (nm)	D value
17.224	2.35	35.70	5.14415
19.12	0.9	93.45	4.63676
26.54	0.9	94.69	3.35518
28.81	1.2	47.57	3.095628
29.77	3.45	24.88	2.99773

32.31	3.45	25.03	2.76774
34.80	0.85	102.86	2.57549
36.53	1.0	87.34	2.457757
38.78	1.05	83.74	2.319946
39.55	0.95	92.78	2.276645
41.72	0.8	110.95	2.162878
44.94	0.7	128.23	2.015049
47.17	0.8	113.13	1.925

IV. CONCLUSION

The biosynthesis of AgNPs from *C.cuspidatus* (Nees & Mart) leaf extract was carried out in this study. Start with a phytochemical analysis of silver nanoparticle extract from *C.cuspidatus* leaves, which revealed the presence of various components. A GC-MS study of AgNPs leaf extract is shown next, which uncovers diverse silicon compounds, carboxylic acid, and heterocyclic compounds. Furthermore, the U.V. study interprets the peak at 192nm to 210nm, leading to a high absorbance spectrum and FTIR with distinct functional groups, stretching and bending. Also, characterization of leaf extract with SEM, XRD, particle size and zeta potential analyzer have been studied. Additionally, this technique could be easily scaled up for industrial applications to considerably enhance the yield of nanoparticles, ensuring its commercial viability in medicine and for commercial purposes.

REFERENCES

Akbari, B., Tavandashti, M. P., & Zandrahimi, M. (2011). Particle size characterization of nanoparticles–a practical approach. *Iranian Journal of Materials Science and Engineering*, *8*(2), 48-56.

Azra, B. H., & Bhavani, D. N. L. (2022, January). Chamaecostus cuspidatus (Nees & Mart.) ethanolic extract: GC-MS analysis and characterization by FTIR and U.V. Retrieved February 9, 2022, from https://ijsdr.org/papers/IJSDR2201012.pdf

Iheagwam, Franklyn Nonso, et al. "GC-MS Analysis and Inhibitory Evaluation of Terminalia Catappa Leaf Extracts on Major Enzymes Linked to Diabetes." *Evidence-Based Complementary and Alternative Medicine*, vol. 2019, pp. 1–14. *Crossref*, https://doi.org/10.1155/2019/6316231.

John, B. I. J. U., T, Sulaiman. C., George, Sateesh., & Reddy, V. R. K. (2014, May 21). *Spectrophotometric estimation of total alkaloids in selected Justicia species*. Innovare Academic Sciences. Retrieved March 17, 2022, from https://innovareacademics.in/journal/ijpps/Vol6Issue5/9556.pdf

Jyoti, Kumari, et al. "Characterization of Silver Nanoparticles Synthesized Using Urtica Dioica Linn. Leaves and Their Synergistic Effects with Antibiotics." *Journal of Radiation Research and Applied Sciences*, vol. 9, no. 3, 2016, pp. 217–27. *Crossref*, https://doi.org/10.1016/j.jrras.2015.10.002.

Mudalige, T. (2019, January 1). *Characterization of Nanomaterials: Tools and Challenges*. ScienceDirect. https://www.sciencedirect.com/science/article/pii/B9780128141304000117

Muthukrishnan, S., Bhakya, S., Senthil Kumar, T., & Rao, M. (2015). Biosynthesis, characterization and antibacterial effect of plant-mediated silver nanoparticles using Ceropegia thwaitesii – An endemic species. *Industrial Crops and Products*, *63*, 119–124. https://doi.org/10.1016/j.indcrop.2014.10.022

Sinha, Sankar Narayan, and Dipak Paul. "Photosynthesis of Silver Nanoparticles UsingAndrographis PaniculataLeaf Extract and Evaluation of Their Antibacterial Activities." *Spectroscopy Letters*, vol. 48, no. 8, 2015, pp. 600–04. *Crossref*, https://doi.org/10.1080/00387010.2014.938756.

Sucheta, Tahlan, S., & Verma, P. K. (2017). Biological potential of thiazolidinedione derivatives of synthetic origin. *Chemistry Central Journal*, *11*(1). https://doi.org/10.1186/s13065-017-0357-2

Suresh, Joghee, et al. "Green Synthesis and Characterization of Zinc Oxide Nanoparticle Using Insulin Plant (Costus Pictus D. Don) and Investigation of Its Antimicrobial as Well as Anticancer Activities." *Advances in Natural Sciences: Nanoscience and Nanotechnology*, vol. 9, no. 1, 2018, p. 015008. *Crossref*, https://doi.org/10.1088/2043-6254/aaa6f1.

What is X-Ray Diffraction Analysis (XRD), and How Does it Work? (n.d.). TWI. Retrieved April 7, 2022, from https://www.twi-global.com/technical-knowledge/faqs/x-ray-diffraction.

Yin, Iris Xiaoxue, et al. "The Antibacterial Mechanism of Silver Nanoparticles and Its Application in Dentistry ." *International Journal of Nanomedicine*, vol. Volume 15, 2020, pp. 2555–62. *Crossref*, https://doi.org/10.2147/ijn.s246764.

Zhang, Xi-Feng, et al. "Silver Nanoparticles: Synthesis, Characterization, Properties, Applications, and Therapeutic Approaches." *International Journal of Molecular Sciences*, vol. 17, no. 9, 2016, p. 1534. *Crossref*, https://doi.org/10.3390/ijms17091534.